Structural and vibrational behaviour of fluorapatite with pressure. Part II: In situ micro-Raman spectroscopic investigation

Article *in* Physics and Chemistry of Minerals · May 2001

DOI: 10.1007/s002690100155

CITATIONS
47

READS
172

3 authors, including:

Paola Comodi
Università degli Studi di Perugia
123 PUBLICATIONS **1,511** CITATIONS

SEE PROFILE

Maria Luce Frezzotti
Università degli Studi di Milano-Bicocca
137 PUBLICATIONS **3,734** CITATIONS

SEE PROFILE

Phys Chem Minerals (2001) 28: 225–231

ORIGINAL PAPER

P. Comodi · Yu Liu · M. L. Frezzotti

Structural and vibrational behaviour of fluorapatite with pressure. Part II: in situ micro-Raman spectroscopic investigation

Received: 25 April 2000 / Accepted: 20 December 2000

Abstract High-pressure Raman investigations were carried out on a synthetic fluorapatite up to about 7 GPa to analyse the behaviour of the phosphate group's internal modes and of its lattice modes. The Raman frequencies of all modes increased with pressure and a trend toward reduced splitting was observed for the PO_4-stretching modes [($v_{3a}(A_g)$ and $v_{3b}(A_g)$; $v_{3a}(E_{2g})$ and $v_{3b}(E_{2g})$] and the PO_4 out-of-plane bending modes [$v_{4a}(A_g)$ and $v_{4b}(A_g)$]. The pressure coefficients of phosphate modes ranged from 0.0047 to 0.0052 GPa^{-1} for v_3, from 0.0025 to 0.0044 GPa^{-1} for v_4, from 0.0056 to 0.0086 GPa^{-1} for v_2 and 0.0046 for v_1 GPa^{-1}, while the pressure coefficients of lattice modes ranged from 0.0106 to 0.0278 GPa^{-1}. The corresponding Grüneisen parameters varied from 0.437 to 0.474, 0.428, 0.232 to 0.409 and 0.521 to 0.800 for phosphate modes v_3, v_1, v_4, v_2, respectively, and from 0.99 to 2.59 for lattice modes. The vibrational behaviour was interpreted in view of the high-pressure structural refinement performed on the same crystal under the same experimental conditions. The reduced splitting may thus be linked to the reduced distortion of the environment around the phosphate tetrahedron rather than to the decrease of the tetrahedral distortion itself. Moreover, the amount of calcium polyhedral compression, which is about three times the compression of phosphate tetrahedra, may explain the different Grüneisen parameters.

P. Comodi (✉)
Dipartimento di Scienze della Terra, Università di Perugia,
Piazza Università, 06100 Perugia, Italy
Tel.: +39-075-5852656; Fax: +39-075-5852603
e-mail: Comodip@unipg.it

Yu Liu
Wuhan Institute of Chemical Technology, Wuhan,
430074 Hubei, PR China

M. L. Frezzotti
Dipartimento di Scienze della Terra, Via Laterina 8,
53100 Siena, Italy

Key words Apatite · Micro-Raman spectroscopy · High pressure

Introduction

Apatite group minerals include fluorapatite, chlorapatite and hydroxyapatite end members. Owing to their wide application in the fields of Earth science, material science and industries, studies on the crystal chemistry of apatite minerals have been especially active (e.g. see review of Elliot 1998).

The application of pressure can produce major changes in crystal structure with regard to bond length and separation of atomic groups. Since diamond-anvil cells (DAC) have made optical spectroscopy under high pressure an accurate, quantitative technique, several investigations of apatites under hydrostatic pressure have recently been reported (Williams and Knittle 1996; Brunet et al. 1999). In their Raman studies of fluorapatite, Williams and Knittle (1996) measured the infrared and Raman spectra of fluorapatite up to pressures of 25 GPa. They found that both site-group and factor-group splittings of the phosphate group's vibrations decrease with compression. A structural evolution with pressure was tentatively proposed to interpret the vibrational data. The anomalous decrease in Davydov splitting under compression was hypothetically associated with the decreased distortion of the environment surrounding the PO_4^{-3} tetrahedron. However, available structural determinations under pressure were lacking, leaving many problems open. Questions such as how the tetrahedra themselves behave in relation to the surrounding environment and what the amount of compression of Ca polyhedra is, remained unanswered.

Moreover, Williams and Knittle (1996) did not measure the shift of lattice modes with pressure or the vibrations associated with calcium. For this reason, bulk Grüneisen parameters of apatite could also not be determined.

In this study new data are presented on the single-crystal polarised Raman spectra of apatite, devoting close attention to lattice modes as well as to the effect of pressure up to 7 GPa on these spectra. This information is used in conjunction with single-crystal X-ray diffraction at high pressure performed on the same crystal using the same high-pressure instrument (Comodi et al. 2001 this issue) to explain the evolution of vibrational modes in terms of structural evolution. Moreover, the structural evolution with pressure, together with the evolution of vibrational spectra, constitutes the basis for the determination of appropriate Grüneisen parameters, which, in turn, provide the basis for the determination of fundamental thermodynamic parameters.

Experiments

Micro-Raman spectroscopy

Several chips from the synthetic fluorapatite sample described in Comodi et al. (2001, this issue) were selected for the micro-Raman investigation. The single crystals were previously oriented with X-ray diffraction and then cut carefully.

Polarised Raman spectra were obtained at the University of Siena with a Jobin-Yvon LTD confocal Labram multichannel spectrometer equipped with a charge-coupled device detector. Raman scattering was excited with the 514.5-nm line of a polarised argon ion laser using 180° backscattering geometry. The incident laser-beam power was 670 mW and was focused to a diameter of approximately 10 μm using an Olympus 10× lens. No thermal effects were detected on the sample. Raman intensity was collected with a Peltier-cooled CCD detector. The scattered light was analysed using a Notch holographic filter with a spectral resolution of 1.5 cm^{-1} and a grating of 1800 grooves mm^{-1}.

Before performing high-pressure measurements, polarised Raman spectra were measured under room conditions in the $X(Y_Z^Y)\bar{X}$, $X(Z_Z^Y)\bar{X}$ and $Z(X_Y^X)\bar{Z}$ orientations for mode assignment and comparison purposes (see Rousseau et al. 1981 for selection rules and Damen et al. 1966 for oriented geometry).

A piece of fluorapatite crystal was placed in a Merrill-Bassett cell, using a 4:1 methanol:ethanol mixture as the pressure-transmitting medium. An Inconel, 250-μm-thick, 750× foil was used as gasket material. Pressure was monitored by measuring the shift of the luminescence line at 6876 Å of Sm^{2+} in a matrix of BaFCl (Comodi and Zanazzi 1993). Polarised spectra were collected with the crystal mounted in the same way as for X-ray diffraction determination. Additionally, the polarised spectra under the geometry of $Z(X_Y^X)\bar{Z}$ were measured at room temperature up to about 5 GPa with the same Labram microspectrometer instrument and compared with the spectra obtained under room conditions, in order to determine the evolution of the low-frequency band, under 400 cm^{-1}, which was particularly evident under this orientation.

Reference spectra from the Merrill-Bassett diamond-anvil cell plus pressure-transmitting methanol–ethanol liquids were collected in the range 100–1700 cm^{-1}, to determine possible interference with the apatite spectra. No fluorescence effects were produced from the diamonds or from the ethanol–methanol mixture. Only the bands at 900, 1042 and 1475 cm^{-1} were ascribed to fluid mixture and the band at 1300 cm^{-1} to the diamonds, and these were always eliminated from the spectra of the sample. On the other hand, important fluorescence effects from the Sm^{2+}:BaFCl were detected: thus, the spectra of the sample were all collected at a distance of more than 100 μm from Sm^{2+}-bearing chips.

Results under room conditions

The fluorapatite structure belongs to the $P6_3/m$ space group with $Z = 2$ (Naray-Szabo 1930), and can be schematised with Ca1 and Ca2 polyhedra forming channels around the central [001] hexad. The coordination numbers for Ca1 and Ca2 are nine- and seven fold, respectively. In the unit cell, 4 Ca1 ions occupy the C_3 site, and 6 Ca2 and 6 P ions are located on symmetry plane *m*. Among the 24 O ions, 6 O1 and 6 O2 lie on the *m* plane and 12 O3 ions occupy the C_i inversion site. F ions are arranged in the channel on the six fold screw axes. Isolated PO_4 tetrahedra connect the Ca polyhedra. According to the factor group theoretical prediction based on the $P6_3/m$ space group (C_{6h}^2), the fluorapatite structure yields the following Raman active vibrations:

$$\Gamma = 12A_g + 16E_{1g} + 26E_{2g} \ .$$

Thus, a total of 54 vibrational modes are predicted. Among these, the phosphate tetrahedron will share the following internal vibrations (Klee 1970):

$$\Gamma(PO_4 \text{ internal}) = 6A_g + 3E_{1g} + 6E_{2g} \ .$$

External vibrations include translation modes and PO_4 libration modes. Their irreducible representations can be expressed as:

$$\Gamma(PO_4 \text{ translations}) = 5A_g + 6E_{2g} + 3E_{1g}$$

$$\Gamma(PO_4 \text{ librations}) = 1A_g + 1E_{2g} + 2E_{1g} \ .$$

The polarised Raman spectra of fluorapatite under room conditions are shown in Fig. 1. The number of apatite Raman modes observed is far fewer than predicted, because of the low Raman intensity of some modes and orientation effects. From Fig. 1, 12 Raman active vibrations can be accounted to the phosphate modes: 1082, 1066, 1054, 1042 and 1035 cm^{-1} for v_3; 965 cm^{-1} for v_1, 616, 606, 591, 581 cm^{-1} for v_4 and 445, 430 cm^{-1} for v_2. These phosphate tetrahedral vibrations demonstrate the main Raman characteristics of apatite minerals and have been fully investigated (Klavitz et al. 1968; Klee 1970; Liu et al. 1998). Owing to the strong luminescence effect and their low intensities, lattice modes deriving from the vibrations of Ca–O and Ca–F bonds below 400 cm^{-1} have hardly been observed before. However, from the oriented spectra measured under room conditions (Fig. 1), it is interesting to note that, besides the above-mentioned phosphate vibrations, some peaks clearly occur under 400 cm^{-1}. Since no impurities were found in our sample, it is reasonable to assign these peaks to the lattice modes resulting from Ca1–O and Ca2–O(F) bonds.

For the Raman spectra recorded under 180° backscattering geometry, the following directional dependence of the different Raman bands can be described (Nasdala 1992). In the geometry of $Z(X_Y^X)\bar{Z}$, the crystal was put on its (001) plane (*xy* plane) with the crystal-

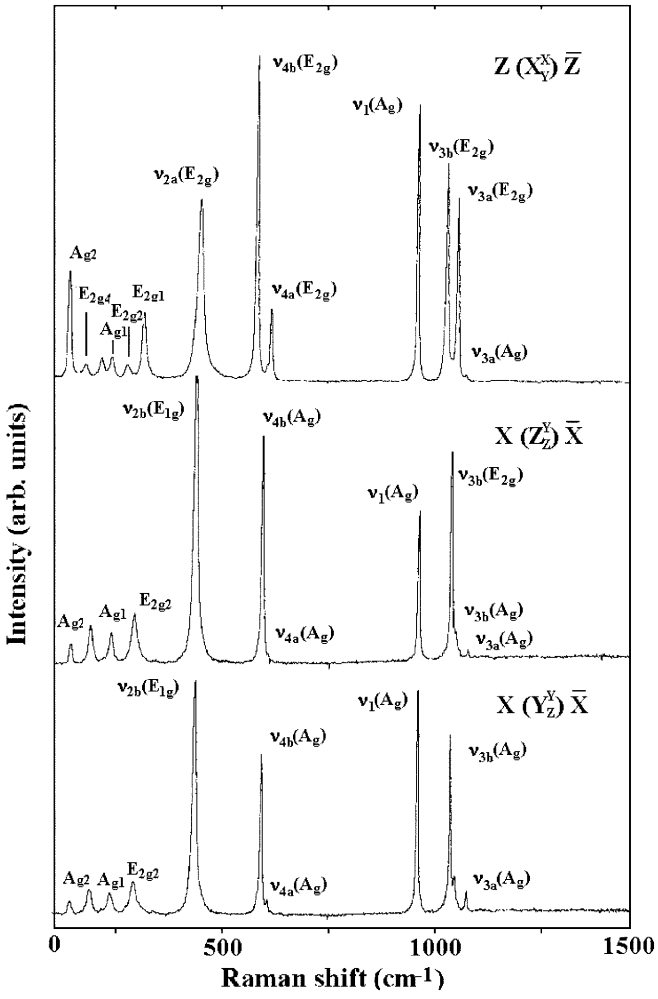

Fig. 1 Polarised Raman spectra of fluorapatite under room conditions

lographic *c* axis parallel to the direction of the laser light beam. In other words, the incidental and scattered vectors of the laser beams were directions Z and −Z, respectively. The polarised direction of the light is parallel to the *a*-axis direction, expressed as X. In this geometry, only A_g and E_{2g} modes can be measured, while the E_{1g} mode is forbidden. In the geometry of $X(Z_Z^Y)\bar{X}$, only A_g and E_{1g} modes can be resolved and E_{2g} is forbidden. On the other hand, in the geometry of $X(Y_Z^Y)\bar{X}$, one can expect to observe all A_g, E_{1g} and E_{2g} Raman active modes, although some of them are so weak that they could be overlapped by the stronger ones. Examination of the three oriented spectra (Fig. 1) led to an easy assignment of all PO_4 internal modes (see Tables 1, 2, 3). The lattice vibrations under 400 cm^{-1} can be logically assigned by carefully comparing the room-oriented data in Table 4. The peaks at 313, 273, 213 and 174 cm^{-1} occur only in the geometry $Z(X_Y^X)\bar{Z}$ and can be assigned to the E_{2g1}, E_{2g2}, E_{2g3}, E_{2g4} modes, respectively. The peaks at 287, 182 cm^{-1} are observed in the orientation $X(Y_Z^Y)\bar{X}$ and $X(Z_Z^Y)\bar{X}$ only, and are forbidden in the geometry $Z(X_Y^X)\bar{Z}$, so they are E_{1g}. The peaks at 231 and near 135–140 cm^{-1} are observed in all three orientations and may be linked to the A_{g1}, A_{g2} modes.

Results under high-pressure conditions

Figure 2a provides some representative spectra of fluorapatite under pressure and Tables 1, 2 and 3 illustrate the shift of Raman frequencies under pressure with related mode assignments. All Raman modes shifted linearly and continuously under the pressure range investigated. Figure 2b shows the shift with pressure of the low frequency modes, whereas Fig. 3 shows the pressure-dependance of all Raman bands.

The compressibility coefficients of PO_4 modes (Table 4) indicate that v_3 and v_1 peaks in the higher-frequency region were more sensitive to pressure compared to the v_4 peaks in the lower-frequency region. In fact, the average compressibility of v_3 and v_1 modes is

Table 1 High-frequency phosphate modes at different pressures (cm^{-1})

Orientation	*P*(GPa)	Phosphate mode					
		$v_{3a}A_g$	$v_{3a}E_{2g}$	$v_{3b}A_g$	$v_{3c}E_{1g}$	$v_{3b}E_{2g}$	$v_1(A_g + E_{2g})$
$X(Y_Z^Y)\bar{X}$	0.0001	1081		1054	1042		965
$X(Z_Z^Y)\bar{X}$	0.0001	1082			1044		964
$Z(X_Y^X)\bar{Z}$	0.0001	1082	1060			1035	965
Random	0.2	1081		1053		1035	965
$Z(X_Y^X)\bar{Z}$	0.83	1085	1065			1039	968
Random	0.99	1090		1062		1040	973
$Z(X_Y^X)\bar{Z}$	2.41	1093	1073			1049	976
Random	3.04	1097		1069		1054	979
Random	3.1	1098		1071		1054	980
$Z(X_Y^X)\bar{Z}$	3.98	1103	1080			1056	983
$Z(X_Y^X)\bar{Z}$	4.24	1104	1083			1060	985
Random	4.72	1105		1081		1060	988
$Z(X_Y^X)\bar{Z}$	4.93	1106	1084			1061	987
Random	5.17	1110		1084		1066	990
Random	6.89	1116		1088		1070	995
Random	7.23	1117		1091		1072	997

Table 2 Low-frequency phosphate modes at different pressures (cm^{-1})

Orientation	P(GPa)	Phosphate mode					
		$\nu_{4a}E_{2g}$	$\nu_{4a}A_g$	$\nu_{4b}A_g$	$\nu_{4b}E_{2g}$	$\nu_{2a}E_{2g}$	$\nu_{2b}E_{1g}$
$X(Y_Z^Y)\bar{X}$	0.0001		606	591			431
$X(Z_Z^Y)\bar{X}$	0.0001			590			429
$Z(X_Y^X)\bar{Z}$	0.0001	616	605		581	445	
Random	0.2		606	590	581		
$Z(X_Y^X)\bar{Z}$	0.83	618	607	592	581	447	
Random	0.99		611	597	586	455	439
$Z(X_Y^X)\bar{Z}$	2.41	623	612	596	585	454	
Random	3.04		613	596	585	458	438
Random	3.1		614	598	586	460	439
$Z(X_Y^X)\bar{Z}$	3.98	626	614	601	586	458	
$Z(X_Y^X)\bar{Z}$	4.24	626	616		589	459	
Random	4.72		617	604	590	468	
$Z(X_Y^X)\bar{Z}$	4.93	626	616		588	460	
Random	5.17		618	604	590	470	445
Random	6.89		621	608	590	473	450
Random	7.23		622	609			

Table 3 Lattice modes at different pressures (cm^{-1})

Orientation	P(GPa)	Lattice mode							
		E_{2g1}	E_{1g}	E_{2g2}	A_{g1}	E_{2g3}	E_{1g}	E_{2g4}	A_{g2}
$X(Y_Z^Y)\bar{X}$	0.0001		287		231		182		135
$X(Z_Z^Y)\bar{X}$	0.0001		287		231		182		135
$Z(X_Y^X)\bar{Z}$	0.0001	313		273	236	213		174	140
$Z(X_Y^X)\bar{Z}$	0.83	320		271	237	218		172	139
$Z(X_Y^X)\bar{Z}$	2.41	334		276	242			185	143
$Z(X_Y^X)\bar{Z}$	3.98	349		283	250			190	145
$Z(X_Y^X)\bar{Z}$	4.24	350		286	245			191	147
$Z(X_Y^X)\bar{Z}$	4.72	354		296	253			198	147

0.0048 and 0.0046 GPa^{-1}, respectively, whereas the average compressibility coefficient for ν_4 is 0.0036 GPa^{-1}. The largest effect was observed in the ν_2 modes, with a compressibility coefficient of 0.0066 GPa^{-1}.

A notable aspect of the pressure shift of the tetrahedral bands is the reduction of the splittings with pressure. In particular, splittings between the PO_4-stretching bands [$\nu_{3a}(A_g)$ and $\nu_{3b}(A_g)$; $\nu_{3a}(E_{2g})$ and $\nu_{3b}(E_{2g})$] and between the PO_4 out-of-plane bending modes [$\nu_{4a}(A_g)$ and $\nu_{4b}(A_g)$] decrease with pressure. In their study, William and Knittle (1996) investigated the evolution of Raman spectra up to 25 GPa and observed that these doublets tend to merge into a single peak. Even if we cannot observe the doublet coalescence due to the lower pressure range investigated, our data do enable us to observe the different band gradients. In the doublets mentioned above, the shifts of the lower-frequency bands are always higher than the shifts of the higher-frequency bands. Consequently, their separations tend to decrease with pressure.

Table 4 also shows the coefficients $d\nu/dP$ (cm^{-1} $kbar^{-1}$) of lattice modes. All low-frequency bands less that 400 cm^{-1} were more sensitive to pressure than high-frequency bands. Lattice mode coefficients, in fact, vary from 0.0278(1) cm^{-1} $kbar^{-1}$ of E_{2g1} to 0.0106(1) cm^{-1} $kbar^{-1}$ of A_{g2}, much more than shifts in phosphate groups.

The pressure coefficients of different Raman modes can be used to obtain the Grüneisen parameters which are extensively required in theoretical calculations. The Grüneisen parameter for the i-th mode is calculated with the equation:

$$\gamma_i = (\delta\nu_i/\delta P)K/\nu_i \ ,$$

where ν_i is the frequency of the i-th mode, K is the bulk modulus. We used a zero pressure isothermal bulk modulus, K_0, of 93 GPa (Comodi et al. 2001, this issue).

The average value for the mode Grüneisen parameters (Table 4) of the bands associated to phosphate group vibrations is 0.44, which comes very close to the value found by Williams and Knittle (1996). On the other hand, the average value for five lattice modes is 1.68, about four times larger than the average phosphate mode.

Discussion and conclusions

The examination of the Raman spectra at different pressures and the comparison with high-pressure struc-

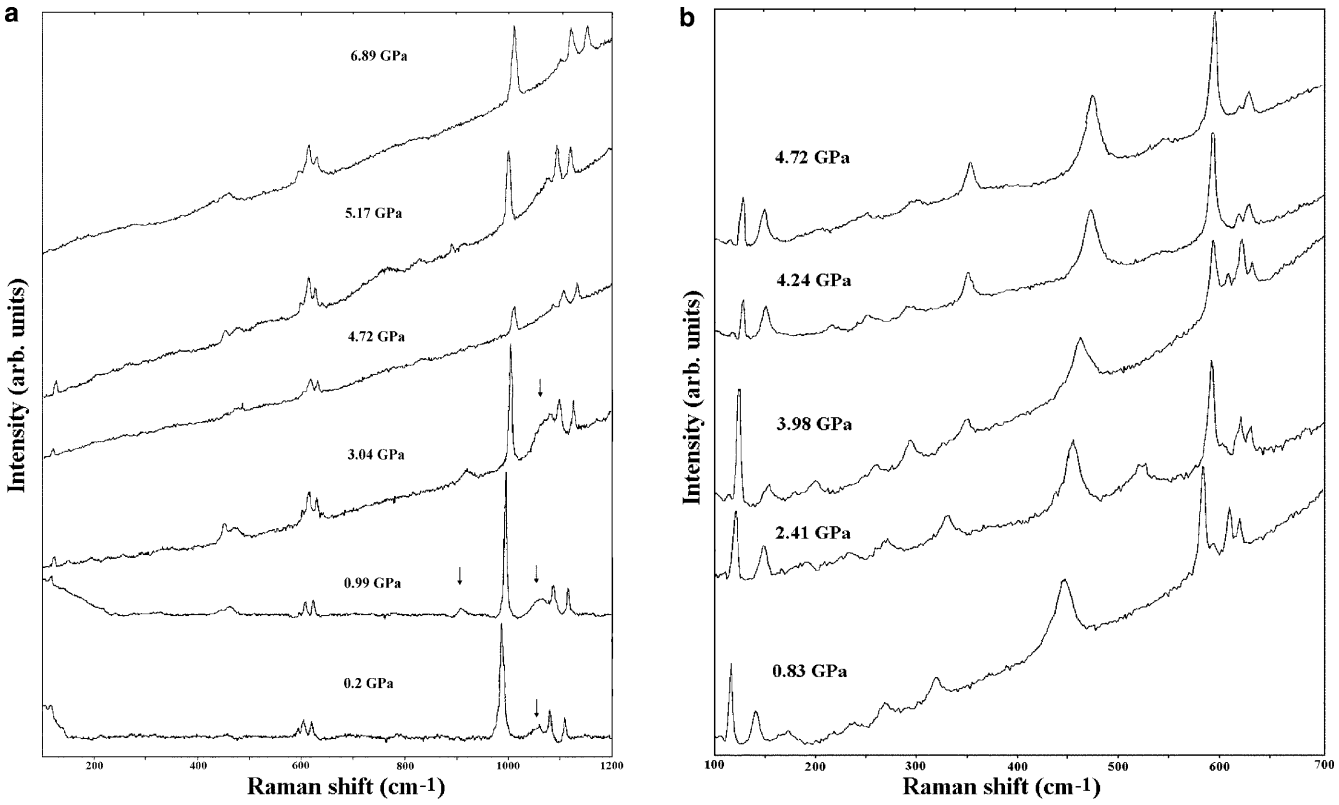

Fig. 2 **a** High-frequency region Raman spectra of fluorapatite at different pressures. The *arrows* indicate the bands at 900 and 1042 cm^{-1} ascribed to the ethanol:methanol mixture. **b** Low-frequency region Raman spectra of fluorapatite at different pressures

tural data obtained from the same sample under the same experimental conditions lead to the following considerations:

1. Both the internal modes of phosphate tetrahedron and lattice modes behave in a linear and continuous fashion when exposed to pressures up to about 7 GPa. Therefore, their vibrational behaviour indicates that fluorapatite does not exhibit any phase transition, not even under the highest pressures reached in the present investigation. This conclusion is in line with the X-ray diffraction study results of Brunet et al. (1999) and Comodi et al. (2001, this issue).

2. The decrease in splitting of the v_3- and v_4-derived bands might be attributed both to the decrease in the overall distortion of the phosphate group and to the reduced distortion of the phosphate group's site symmetry. High-pressure refinements (Comodi et al. 2001, this issue) allow us to identify the real cause of splitting reduction. In fact, the comparison of the refinements under room conditions and at high pressures shows that the calcium polyhedra become more regular with pressure, whereas the phosphate tetrahedron distortion remains unchanged. Thus, the decrease in v_3 and v_4 mode splitting must be associated to the reduced distortion in the environment around the PO_4 tetrahedra.

3. The average value of the phosphate group mode Grüneisen parameters is relatively low compared to the value of bulk Grüneisen parameters found for relatively incompressible oxide crystals without polymerised tetrahedra and ranging between 0.8 and 2. Such low Grüneisen parameter values of the vibration linked to isolated tetrahedra had already been examined by Knittle and Williams (1993) for silicate. The evolution of the tetrahedral mode is not, in fact, representative of the structural evolution on the whole, yet it appears that the lattice modes and the vibration associated to the calcium polyhedra strongly affect the bulk Grüneisen parameter. In fact, the Grüneisen parameters of the vibration associated to lattice modes varied from 0.99 to 2.59 (Table 4), which are two to four times larger than phosphate parameters. This implies that, under pressure, the behaviour of a Ca–O(F) polyhedra is much less rigid than that of the phosphate tetrahedron. In this case as well, the comparison with the X-ray diffraction results improves the interpretation of the Raman spectra evolution. The high-pressure single-crystal refinements (Comodi et al. 2001, this issue) showed that the calcium polyhedra were much more compressible than the phosphate tetrahedra. The bulk moduli of phosphate tetrahedron of Ca1 and Ca2 polyhedra were 270(10), 100(4), 86(3) GPa, respectively.

The Grüneisen parameters of the single Raman modes may be used to determine the average Grüneisen parameter $\langle\gamma\rangle$, which is entered in the formulation of the volume constant heat capacity C_v, expressed as $\alpha V/K\gamma$, where α is the thermal expansion, V is the molar volume

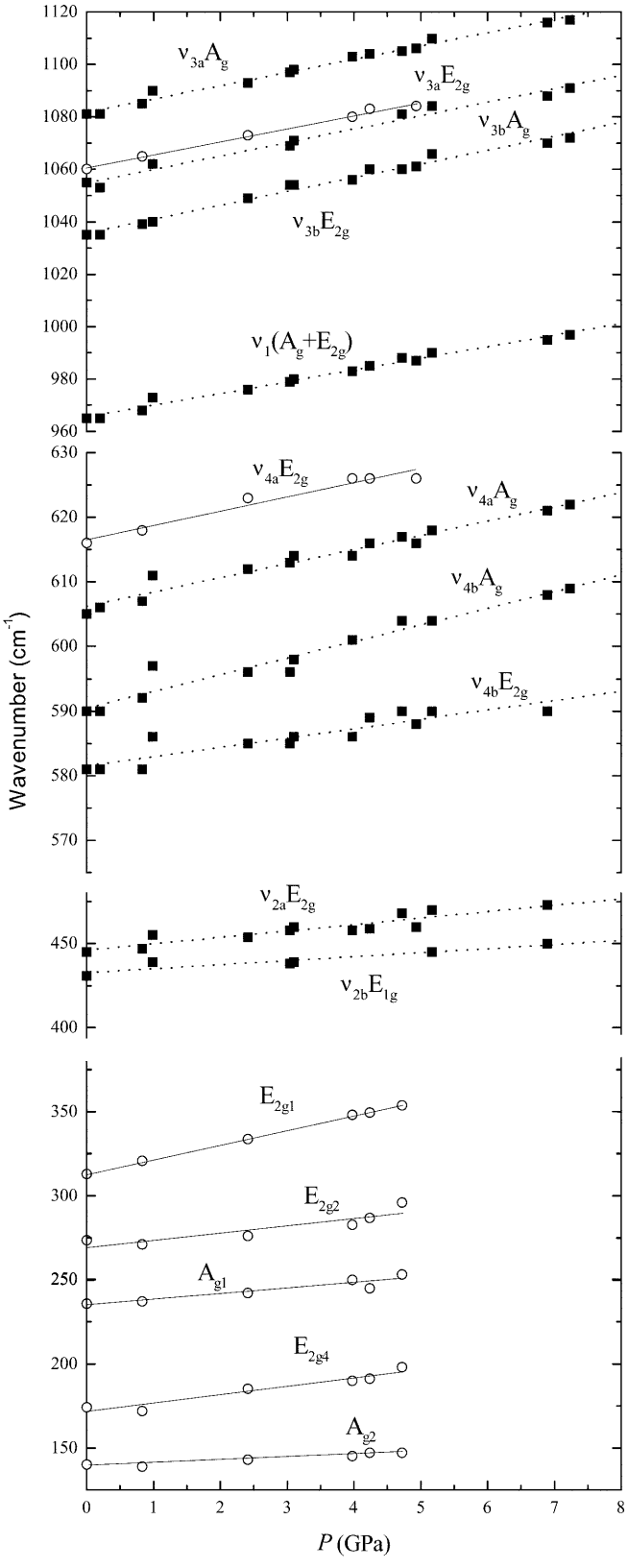

Fig. 3 Pressure dependence of fluorapatite Raman bands. The *lines* are linear regression to the data. *Dashed lines* and *full squares* refer to the Raman bands collected with random orientation; *full lines* and *open circles* refer to the Raman bands collected under $Z(X_Y^X)\bar{Z}$ orientation

Table 4 Raman frequency shifts with pressure. v_0 and β represent the parameters in the expressions: $v_P = v_0(1 + \beta P)$, where v_P and v_0 are in cm^{-1} and β are in GPa^{-1}. Grüneisen parameters were calculated assuming $K_0 = 93$ GPa. (Comodi et al. 2001)

	v_0	β	R	Grüneisen parameter
Phosphate modes				
$v_{3a}(A_g)$	1080.3(5)	0.0047(2)	0.996	0.437
$v_{3a}(E_{2g})$	1060.5(6)	0.0047(2)	0.997	0.437
$v_{3b}(A_g)$	1052.0(7)	0.0049(3)	0.998	0.456
$v_{3b}(E_{2g})$	1034.7(9)	0.0051(5)	0.992	0.474
$v_1(A_g+E_{2g})$	964.3(4)	0.0046(2)	0.997	0.428
$v_{4a}(E_{2g})$	615.9(6)	0.0040(3)	0.987	0.372
$v_{4a}(A_g)$	605.4(5)	0.0036(3)	0.981	0.335
$v_{4b}(A_g)$	589.3(6)	0.0044(3)	0.986	0.409
$v_{4b}(E_{2g})$	580.3(4)	0.0025(3)	0.983	0.232
$v_{2a}(E_{2g})$	444.2(9)	0.0086(9)	0.930	0.800
$v_{2b}(E_{1g})$	431.2(2)	0.0056(9)	0.92	0.521
Lattice mode				
E_{2g1}	312.8(3.2)	0.0278(4)	0.979	2.59
E_{2g2}	268.9(3.8)	0.0126(3)	0.879	1.17
A_{g1}	234.5(1.8)	0.0133(2)	0.964	1.24
E_{2g4}	170.8(2.1)	0.0260(2)	0.971	2.42
A_{g2}	138.2(7)	0.0106(1)	0.976	0.99

and K is the bulk modulus. Calculation of $\langle\gamma\rangle$ passes through the analysis of the density of states, which is beyond the scope of this paper. Lattice dynamics calculation on fluorapatite would therefore be welcomed.

Acknowledgements We are indebted to Dr. P. Yang, the donor of the fluorapatite sample. The Department of Earth Sciences of Siena with a micro-Raman spectrograph funded by the Italian Antarctic National Project (PNRA) is acknowledged. Prof. P. F. Zanazzi and Prof. E. Castellucci are thanked for their critical comments on the manuscript. Many thanks are due H. A. Giles (MA) for editing the English. The Italian MURST provided support for this research through grants to Prof. P. F. Zanazzi (project: Transformation, reactions, ordering in minerals). The financial support from FARCB197, CNR 97.00251 to Prof. Stoppa and from Hubei Educational Department (grant no. 99A122) to L.Y. are acknowledged.

References

Brunet F, Allan DR, Redfern SAT, Angel RJ, Miletich RM, Reichmann HJ, Sergent J, Hanfland M (1999) Compressibility and thermal expansivity of synthetic apatites, $Ca_5(PO_4)_3X$ with X = OH, F and Cl. 1999. Eur J Mineral 11: 1023–1035

Comodi P, Zanazzi PF (1993) Improved calibration curve for the Sm^{2+}:BaFCl pressure sensor. J Appl Crystallogr 26: 843–845

Comodi P, Liu Y, Zanazzi PF, Montagnoli M (2001) Structural and vibrational behaviour of fluorapatite with pressure. Part I: in situ single-crystal X-ray diffraction investigation. Phys Chem Miner (this issue)

Damen TC, Porto SPS, Tell B (1966) Raman effect in zinc oxide. Phys Rev 142(2): 570–574

Elliot JC (1998) Recent studies of apatites and other calcium orthophosphates. Proceedings Calcium phosphate materials. Fundamentals. Berck sur Mer, France, 1997. Sauramps Med Ed pp 25–66

Klee W (1970) The vibrational spectra of the phosphate ions in fluorapatite. Zeit Kristallogr 131: 95–102

Knittle E, Williams Q (1993) High-pressure Raman spectroscopy of $ZrSiO_4$: observation of the zircon to scheelite transition at 300 K. Am Mineral 78: 245–252

Klavitz LC, Kingsley J, Elkin EL (1968) Raman and infrared studies of coupled PO_4^{-3} vibrations. J Chem Phys 49(10): 4600–4610

Liu Y, Comodi P, Sassi P (1998) Vibrational spectroscopic investigation of phosphate tetrahedron in fluor-, hydroxy-, and chlorapatites. N Jb Miner Abh 174(2): 211–222

Nàray-Szabò S (1930) The structure of apatite. Zeit Kristallogr 75: 387–398

Nasdala L (1992) A Raman study on the so-called pseudoapatite from Halsbrucke near Freiberg/Saxony. N Jb Miner Abh 164: 211–227

Rousseau DL, Baumann RP, Porto SPS (1981) Normal mode determination in crystal. J Raman Spectrosc 10(1): 253–290

Williams Q, Knittle E (1996) Infrared and raman spectra of $Ca_5(PO_4)_3F$-fluorapatite at high pressure: compression-induced changes in phosphate site and Davydov splittings. J Phys Chem Solid 57(4): 417–422